Perturbative versus Schwinger-propagator method for the calculation of amplitudes in a magnetic field

José F. Nieves

Laboratory of Theoretical Physics, Department of Physics, P.O. Box 23343, University of Puerto Rico, Río Piedras, Puerto Rico 00931-3343

Palash B. Pal

Saha Institute of Nuclear Physics, 1/AF Bidhan-Nagar, Calcutta 700064, India
(Received 9 March 2006; published 3 May 2006)

We consider the calculation of amplitudes for processes that take place in a constant background magnetic field, first using the standard method for the calculation of an amplitude in an external field, and second utilizing the Schwinger propagator for charged particles in a magnetic field. We show that there are processes for which the Schwinger-propagator method does not yield the total amplitude. We explain why the two methods yield equivalent results in some cases and indicate when we can expect the equivalence to hold. We show these results in fairly general terms and illustrate them with specific examples as well.

I. INTRODUCTION

In this paper we are concerned with the calculation of amplitudes for processes that take place in a constant background magnetic field B. There are many papers in the literature in which this kind of process are considered [1–11], a significant fraction of which have to do with neutrino processes that may take place in a variety of astrophysical environments. It is useful to keep those particular situations in mind, but for our purposes it is convenient to set up a more general framework.

Thus, let us suppose that we want to calculate the amplitude for the transition

$$|i\rangle \xrightarrow{B} |f\rangle, \tag{1.1}$$

where $|i\rangle$ and $|f\rangle$ denote two states, and the letter B above the arrow indicates that the transition takes place in the presence of the external magnetic field. For reasons that will become clear below, we restrict the initial and final states to contain no charged particles, only neutral ones, and we consider the calculation of the amplitude up to terms linear in B.

There are at least two ways to proceed with such a calculation. One way is to start by computing in standard Feynman diagram perturbation theory the Green's function for

$$|i + \gamma\rangle \rightarrow |f\rangle, \tag{1.2}$$

in the absence of B, and, in particular, with the photon off-shell, which corresponds to the matrix element $\langle f|j_\mu|i\rangle$ of the electromagnetic current. Since the external particles are assumed to be neutral, then in the context of the perturbative calculation the off-shell photon is attached only to the internal lines of any diagram that contributes to the Green's function. The amplitude for the transition in Eq. (1.1) is then obtained at the end by inserting the appropriate photon

field that corresponds to the background magnetic field, together with the wave functions of the particles in the initial and final states involved in the transition. This procedure yields the amplitude to first order in B. This was in fact the approach employed in the original calculation of the neutrino index of refraction in the presence of a magnetic field [12]. We will refer to this method as the *Perturbative Method*, or P-method for short.

An alternative approach is to calculate the Green's function for the transition

$$|i\rangle \rightarrow |f\rangle, \tag{1.3}$$

but employing the Schwinger [13] propagator in place of the Feynman propagator for all the charged internal lines that appear in any diagram that contributes to the amplitude. Then, if the result is expanded in powers of B, the conventional expectation is that the linear term in B should coincide with the result of the P-method as specified above. We will refer to the procedure that we have just described as the *Linear Schwinger Method*, or S-method for short.

Indeed, the familiar calculations already mentioned involving neutrino processes confirm this expectation that both methods yield the same result. The question we address here is whether this is a special feature of the processes that have been considered, and whether we can expect the result to hold for any other process of the type we are considering.

The purpose of this paper is to show that there are processes for which this equivalence does not hold. To be specific, in those cases, the diagrams that contribute to the amplitude in the P-method can be classified in two topologically distinct groups that we call type-1 and type-2 diagrams, which are distinguished according to whether the electromagnetic vertex has only internal lines attached to it, or whether it has some external lines attached as well. As we show, the S-method yields a result that is equivalent

to the result of the type-1 diagrams. For processes for which the type-2 diagrams do not exist, both the P and S methods yield the same result, which is the case of the neutrino processes that we have mentioned. But in the more general case in which the type-2 diagrams exist, the S-method does not yield the complete amplitude. The total amplitude is obtained by taking the result of the type-1 diagrams, which can be calculated by either method, and then adding the result of the type-2 diagrams using the P-method.

As already mentioned, we have in mind the type of processes that occur in the context of various astrophysical problems, for which the effects of the background cannot be neglected *a priori*. However, we should stress that in this paper we are concerned with the vacuum amplitudes. That is, we consider the amplitudes in the idealized situation in which, apart from the external magnetic field, the processes take in place in the vacuum. There are several reasons for this. One of them is the fact that, in any case, the vacuum amplitude contributes to the total amplitude that includes the effects of the background. Therefore, in those cases in which the vacuum amplitude is not calculable by the S-method, the total background amplitude is not calculable either. In addition, the method that we develop for the calculation of such amplitudes can be extended to the framework of finite temperature field theory to include the effects of the background medium.

The paper is organized as follows. In Sec. II, we derive the linearized forms of the Schwinger propagators for fermions, scalars, and vector particles in order to set up the stage for calculations in the S-method. In Sec. III, we outline the P approach, introducing the classifications of all relevant diagrams into two types, which we have called type-1 and type-2 above. In Sec. IV, we show the example of a process in which the S- and the P-methods yield identical results because only type-1 diagrams are present. In Sec. V, we discuss processes where type-2 diagrams are also present, so that the S-method does not give the total amplitude. Finally, in Sec. VI, we present our conclusions.

II. LINEAR SCHWINGER APPROACH

The Schwinger formula [13] gives the fermion propagator to all orders in the B field, and the analogous formulas for the scalar and vector propagators are also known [14]. Since we will be looking at the amplitudes calculated to first order in B, a simpler formula, which is correct to that order, is sufficient for our purpose. Below we give a short derivation of the linear formulas for the propagators, in a manner that will be useful in what follows.

A. Fermion propagator in a magnetic field

We follow the derivation given in Ref. [11] for the fermion propagator, and subsequently extend it to obtain the analogous result for the scalar and vector propagator. The propagator of a Dirac particle of mass m and charge

eQ in an external electromagnetic field is

$$[i\gamma^\mu \mathcal{D}_\mu - m]S(x, x') = \delta^4(x - x'), \qquad (2.1)$$

where the electromagnetic gauge covariant (EGC) derivative $\mathcal{D}_\mu$ is defined by

$$\mathcal{D}_\mu = \frac{\partial}{\partial x^\mu} + ieQA_\mu(x). \qquad (2.2)$$

The Schwinger solution is of the form

$$S(x, x') = \Phi(x, x') \int \frac{d^4p}{(2\pi)^4} e^{-ip\cdot(x-x')} S_F(p), \qquad (2.3)$$

where the overall phase $\Phi(x, x')$ is chosen such that

$$i\mathcal{D}_\mu \Phi(x, x') = \frac{eQ}{2} F_{\mu\nu}(x - x')^\nu \Phi(x, x'), \qquad (2.4)$$

and it depends on the gauge choice for the background field. For a constant field $F_{\mu\nu}$ corresponding to the background magnetic field, we can choose the gauge for the vector potential such that

$$A_\mu(x) = -\tfrac{1}{2} F_{\mu\nu} x^\nu. \qquad (2.5)$$

With this choice,

$$\Phi(x, x') = \exp\left(\frac{i}{2} eQ x^\mu F_{\mu\nu} x'^\nu\right), \qquad (2.6)$$

and in a different gauge, the expression for $\Phi(x, x')$ will be different [15,16]. We will always employ the gauge dictated by Eq. (2.5).

By virtue of Eq. (2.4), Φ has the property that, for an arbitrary function f,

$$\mathcal{D}_\mu(\Phi f) = \Phi\left[\partial_\mu - \frac{ieQ}{2} F_{\mu\nu}(x - x')^\nu\right] f. \qquad (2.7)$$

Moreover, if f is a translationally invariant function of two coordinates, $f(x, x')$, so that its Fourier transform is given by

$$f(x, x') = \int \frac{d^4p}{(2\pi)^4} e^{-ip\cdot(x-x')} \tilde{f}(p), \qquad (2.8)$$

then it follows that

$$\mathcal{D}_\mu(\Phi f) = -i\Phi(x, x') \int \frac{d^4p}{(2\pi)^4} e^{-ip\cdot(x-x')} \tilde{\mathcal{D}}_\mu \tilde{f}(p), \qquad (2.9)$$

where

$$\tilde{\mathcal{D}}_\mu = p_\mu - \frac{ieQ}{2} F_{\mu\nu} \frac{\partial}{\partial p_\nu}. \qquad (2.10)$$

Substituting Eq. (2.3) into Eq. (2.1) and using Eq. (2.9), the equation for the momentum-space propagator $S_F(p)$ is

$$\Phi(x, x') \int \frac{d^4 p}{(2\pi)^4} e^{-ip\cdot(x-x')} \left[\not{p} - \frac{ieQ}{2} F^{\mu\nu} \gamma_\mu \frac{\partial}{\partial p^\nu} - m \right]$$
$$\times S_F(p) = \delta^4(x - x'). \qquad (2.11)$$

Using $\Phi(x, x) = 1$ this equation can be solved by setting

$$\left[\not{p} - m - \frac{ieQ}{2} F^{\mu\nu} \gamma_\mu \frac{\partial}{\partial p^\nu} \right] S_F(p) = 1. \qquad (2.12)$$

The exact solution of this equation gives the Schwinger formula. As already mentioned, for our purpose it is enough to obtain the solution only to the linear order in B, and therefore we write it as

$$S_F(p) = S_0(p) + S_B(p), \qquad (2.13)$$

where $S_0(p)$ is the propagator in the vacuum,

$$S_0(p) = \frac{1}{\not{p} - m + i\epsilon}, \qquad (2.14)$$

and $S_B(p)$ is the correction due to the B field. Substituting this form in Eq. (2.12) and solving perturbatively, we then obtain

$$S_B(p) = S_0(p) \left[\frac{ieQ}{2} F^{\mu\nu} \gamma_\mu \frac{\partial}{\partial p^\nu} \right] S_0(p). \qquad (2.15)$$

B. Propagator of scalars and charged gauge bosons in a magnetic field

Following the approach outlined above, we now find the analogous expressions for the propagators of charged gauge bosons and scalars, up to the linear order in B.

The scalar field propagator satisfies the equation

$$[\mathcal{D}^\mu \mathcal{D}_\mu + m^2] \Delta(x, x') = -\delta^4(x - x'). \qquad (2.16)$$

Taking the ansatz

$$\Delta(x, x') = \Phi(x, x') \int \frac{d^4 p}{(2\pi)^4} e^{-ip\cdot(x-x')} \Delta_F(p), \qquad (2.17)$$

the equation for $\Delta_F(p)$ is

$$[\tilde{\mathcal{D}}^\mu \tilde{\mathcal{D}}_\mu - m^2] \Delta_F(p) = 1. \qquad (2.18)$$

Retaining only up to linear terms in B, the equation becomes

$$\left[p^2 - m^2 - ieQ F_{\mu\nu} p^\mu \frac{\partial}{\partial p_\nu} \right] \Delta_F(p) = 1, \qquad (2.19)$$

which we solve by writing

$$\Delta(p) = \Delta_0(p) + \Delta_B(p), \qquad (2.20)$$

with

$$\Delta_0(p) = \frac{1}{p^2 - m^2 + i\epsilon}. \qquad (2.21)$$

Substituting this form in Eq. (2.19) we then obtain for the

B-dependent term

$$\Delta_B(p) = ieQ F_{\mu\nu} p^\mu \Delta_0(p) \frac{\partial}{\partial p_\nu} \Delta_0(p). \qquad (2.22)$$

We consider now the charged gauge bosons. The W-bosons do not have minimal couplings with the photon. In other words, in addition to the couplings obtained by replacing all partial derivatives in their free Lagrangian by the EGC derivative defined in Eq. (2.2), they have an anomalous coupling of the form $W_\mu^\dagger F^{\mu\nu} W_\nu$. Thus, the terms in the pure gauge Lagrangian involving the quadratic terms in W and their couplings to the photon can be written in this suggestive form used by Erdas and Feldman [14]:

$$\mathcal{L}_{WA} = -(\mathcal{D}_\mu W_\nu)^\dagger (\mathcal{D}_\mu W_\nu - \mathcal{D}_\nu W_\mu) + ie W_\mu^\dagger W_\nu F^{\mu\nu}, \qquad (2.23)$$

where W_μ is the field operator which annihilates the W^+ boson. In addition, we need to introduce the gauge fixing terms which are necessary for quantizing the gauge fields. These terms have the generic form

$$\mathcal{L}_{gf} = -\frac{1}{\xi} |f_W|^2, \qquad (2.24)$$

where f_W contains the W-field as well as the unphysical Higgs boson fields. In the commonly used R_ξ gauges, one takes
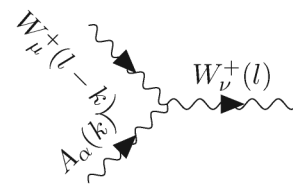
$$f_W = \partial^\mu W_\mu + i\xi M_W \phi^+ \qquad (2.25)$$

so that the gauge fixing Lagrangian contains no interaction term.

In the presence of a background electromagnetic field, however, the pure gauge Lagrangian contains EGC derivatives of W, not simple derivatives. Erdas and Feldman [14] pointed out that it is therefore more convenient that we use a gauge condition that involved $\mathcal{D}_\mu$ and not just ∂_μ acting on the W-boson field. Indeed, such a gauge condition was discussed in a different context much earlier [17] where, instead of Eq. (2.25), the following choice was made:

$$f_W = \mathcal{D}^\mu W_\mu + i\xi M_W \phi^+. \qquad (2.26)$$

The resulting gauge fixing term, defined according to Eq. (2.24), must be added to the gauge-invariant part of the Lagrangian before obtaining Feynman rules. An important consequence of Eq. (2.26) is that the resulting Lagrangian has no cubic coupling involving the W-boson, the unphysical Higgs, and the photon. On the other hand, the Feynman rule for the cubic WW-photon coupling contains the gauge parameter ξ, and is given by

$$= ieO_{\alpha\mu\nu}(k, l - k) \qquad (2.27)$$

with

$$O_{\alpha\mu\nu}(k, l - k) = \eta_{\mu\nu}(2l - k)_\alpha - \eta_{\nu\alpha}((2 - \zeta)k + \zeta l)_\mu$$
$$+ \eta_{\alpha\mu}(2k - \zeta l)_\nu, \qquad (2.28)$$

where $\eta_{\mu\nu}$ is the metric tensor and the shorthand

$$\zeta = 1 - \frac{1}{\xi} \qquad (2.29)$$

has been used.

The equation of motion of the W-bosons in the background field, which is derived from the Lagrangian that follows from Eqs. (2.23) and (2.24), together the gauge fixing function defined by Eq. (2.26), is given by

$$\left[-\eta_{\alpha\beta}(\mathcal{D}^2 + M_W^2) + \mathcal{D}_\alpha\mathcal{D}_\beta - \frac{1}{\xi}\mathcal{D}_\beta\mathcal{D}_\alpha - ieF_{\beta\alpha} \right]W^\alpha$$
$$= 0, \quad (2.30)$$

where the last term comes from the anomalous electromagnetic coupling of the W-bosons that appears in Eq. (2.23). Using the commutation relation

$$[\mathcal{D}_\alpha, \mathcal{D}_\beta]W^\gamma = ieF_{\alpha\beta}W^\gamma, \qquad (2.31)$$

the equation can be rewritten in the form

$$[-\eta_{\alpha\beta}(\mathcal{D}^2 + M_W^2) + \zeta\mathcal{D}_\beta\mathcal{D}_\alpha - 2ieF_{\beta\alpha}]W^\alpha = 0, \qquad (2.32)$$

and the propagator in the coordinate space then satisfies the equation

$$[\eta_{\lambda\mu}(\mathcal{D}^\alpha\mathcal{D}_\alpha + M_W^2) - \zeta\mathcal{D}^\lambda\mathcal{D}^\mu + 2ieF_{\lambda\mu}]D^{\mu\nu}(x, x')$$
$$= \delta_\lambda^\nu\delta^4(x - x'). \qquad (2.33)$$

Following the same procedure used above for the fermion and scalar fields, we obtain the equation for the momentum-space propagator,

$$[\eta_{\lambda\mu}(-\tilde{\mathcal{D}}_\alpha\tilde{\mathcal{D}}^\alpha + M_W^2) + \zeta\tilde{\mathcal{D}}_\lambda\tilde{\mathcal{D}}_\mu + 2ieF_{\lambda\mu}]D_F^{\mu\nu}(p) = \delta_\lambda^\nu, \qquad (2.34)$$

where $\tilde{\mathcal{D}}$ has been defined in Eq. (2.10). Linearization of this equation gives

$$\left[\eta_{\lambda\mu}(-p^2 + M_W^2) + \zeta p_\lambda p_\mu - \frac{ie}{2}F^{\alpha\beta}R_{\alpha\beta\lambda\mu} \right]D_F^{\mu\nu}(p) = \delta_\lambda^\nu, \qquad (2.35)$$

where $R_{\alpha\beta\lambda\mu}$ is defined by

$$R_{\alpha\beta\lambda\mu} = [-2\eta_{\lambda\mu}p_\alpha + \zeta p_\lambda\eta_{\alpha\mu} + \zeta p_\mu\eta_{\alpha\lambda}]\frac{\partial}{\partial p^\beta}$$
$$+ (\zeta - 4)\eta_{\lambda\alpha}\eta_{\mu\beta}, \qquad (2.36)$$

and it can be expressed in the form

$$R_{\alpha\beta\lambda\mu} = -O_{\alpha\lambda\mu}(0, p)\frac{\partial}{\partial p^\beta} + (\zeta - 4)\eta_{\lambda\alpha}\eta_{\mu\beta}, \qquad (2.37)$$

with $O_{\alpha\lambda\mu}$ being the tensor defined in Eq. (2.28). As before, we solve Eq. (2.35) by decomposing the propagator in the form

$$D_F^{\mu\nu}(p) = D_0^{\mu\nu}(p) + D_B^{\mu\nu}(p), \qquad (2.38)$$

where

$$D_0^{\alpha\beta}(p) = \frac{1}{p^2 - M_W^2 + i\epsilon}\left(-\eta^{\alpha\beta} + \frac{(1 - \xi)p^\alpha p^\beta}{p^2 - \xi M_W^2} \right). \qquad (2.39)$$

Then, substituting Eq. (2.38) into Eq. (2.35) and solving for the linear term in B, we obtain

$$D_B^{\mu\nu}(p) = \frac{ie}{2}F^{\alpha\beta}D_0^{\lambda\mu}(p)R_{\alpha\beta\lambda\rho}D_0^{\rho\nu}(p). \qquad (2.40)$$

In the gauge introduced in Eq. (2.26), the propagator of the unphysical charged Higgs field in the background magnetic field, which we denote by $\Delta_F^{(W)}(p)$, can obtained by making the substitution

$$m^2 \rightarrow \xi M_W^2 \qquad (2.41)$$

in the formulas given in Eqs. (2.21) and (2.22) for the scalar propagator. For later reference, we quote the result,

$$\Delta_F^{(W)}(p) = \Delta_0^{(W)}(p) + \Delta_B^{(W)}(p), \qquad (2.42)$$

where

$$\Delta_0^{(W)}(p) = \frac{1}{p^2 - \xi M_W^2},$$
$$\Delta_B^{(W)}(p) = ieQF_{\mu\nu}p^\mu\Delta_0^{(W)}(p)\frac{\partial}{\partial p_\nu}\Delta_0^{(W)}(p). \qquad (2.43)$$

The Fadeev-Popov ghost propagator should also be modified in a magnetic field, but we will not need it in our subsequent discussion.

III. THE PERTURBATIVE APPROACH

Here we consider the calculation of the B-dependent contribution to the off-shell amplitude for the process $i \xrightarrow{B} f$ using the P-method, which we denote by $\mathbb{M}_{i\rightarrow f}^{(P)}$. For clarity, we consider first the case in which i and f are single particle states (e.g., a neutrino) and extend the result afterwards to the general case.

A. One-particle amplitude

In the P-method the amplitude is expressed in terms of the off-shell electromagnetic vertex function $\Gamma_\mu(p_i, p_f)$, which is defined such that the on-shell matrix element of the electromagnetic current operator $j_\mu(x)$ is given by

$$\langle f(p_f)|j_\mu(0)|i(p_i)\rangle = \bar{w}_f\Gamma_\mu(p_i, p_f)w_i, \qquad (3.1)$$

where $w_{i,f}$ denote the momentum-space wave functions appropriate for the particle (e.g., Dirac spinors for fermions, polarization vectors for spin-1 particles). The off-shell amplitude for the transition $i \to f$ in an external electromagnetic field is then given by

$$\mathbb{M}_{i \to f}^{(P)}(p_i, p_f) = -i \int d^4x \, e^{i(p_f - p_i) \cdot x} A^\mu(x) \Gamma_\mu(p_i, p_f),$$

(3.2)

which can be written as

$$\mathbb{M}_{i \to f}^{(P)}(p_i, p_f) = -i \left[\int d^4x \, e^{ik \cdot x} A^\mu(x) \Gamma_\mu(p_i, p_i + k) \right]_{k = p_f - p_i}.$$

(3.3)

For $A(x)$ we now substitute the vector potential given in Eq. (2.5). Then using the representation

$$\delta'(t) = \frac{i}{2\pi} \int_{-\infty}^{+\infty} dz \, z e^{izt}$$

(3.4)

as well as the relation

$$\delta'(t - a)f(t) = -\delta(t - a)f'(a)$$

(3.5)

for the derivative of the delta function, the amplitude is given by

$$\mathbb{M}_{i \to f}^{(P)}(p_i, p_f) = -\frac{1}{2}(2\pi)^4 \delta^4(p_f - p_i) F^{\mu\nu}$$
$$\times \left[\frac{\partial}{\partial k^\nu} \Gamma_\mu(p_i, p_i + k) \right]_{k=0},$$

(3.6)

where in the last factor we have set $k = 0$ by virtue of the delta function. The B-dependent contribution to the self-energy, which is identified by writing

$$\mathbb{M}_{i \to f}^{(P)}(p_i, p_f) = -i(2\pi)^4 \delta^4(p_i - p_f) \Sigma^{(P)}(p_i),$$

(3.7)

is therefore given by

$$\Sigma^{(P)}(p) = -\frac{i}{2} F^{\mu\nu} \left[\frac{\partial}{\partial k^\nu} \Gamma_\mu(p, p + k) \right]_{k=0}.$$

(3.8)

B. General amplitude

We now consider the general case. Suppose the state $|i\rangle$ contains n particles with momenta $p_{1,2,\ldots,n}$, and the state $|f\rangle$ contains n' particles with momenta $p'_{1,2,\ldots,n'}$. We denote the total momenta of each state by

$$P = \sum_{i=1}^{n} p_i, \qquad P' = \sum_{f=1}^{n'} p'_f.$$

(3.9)

In analogy with the one-particle case discussed already, we now define the off-shell vertex function involving the photon in such a way that the on-shell matrix element of the electromagnetic current operator $j_\mu(x)$ between the states $|i\rangle$ and $|f\rangle$ is given by

$$\langle f| j_\mu(0) |i\rangle = (\bar{w}_f)^{\alpha'_1 \cdots \alpha'_{n'}} \Gamma_{\mu\alpha_1 \cdots \alpha_n \alpha'_1 \cdots \alpha'_{n'}}$$
$$\times (p_1, p_2, \ldots, p_n, p'_1, p'_2, \ldots, p'_{n'})(w_i)^{\alpha_1 \cdots \alpha_n},$$

(3.10)

where the middle factor is the vertex function, and the other two factors symbolically denote the collection of momentum-space wave functions from the final and initial state particles. We have put a general kind of index for these external particles. For a scalar in the external states, the corresponding w-factor will be unity, and the index should be absent in the vertex function. For a fermion field, we usually suppress the index in favor of a matrix notation. For vector and tensor fields, the indices appear explicitly. For the moment, we will omit all indices on the vertex function except the photon index, and use the compact notation for the momenta to write just $\Gamma_\mu(p_i, p'_f)$ for the vertex function, but it should be understood to be the full quantity defined above, with all indices and all momenta.

We classify the diagrams that contribute to the vertex function into two types. As stated in the Introduction, we deal with processes where all particles in external states are electrically neutral. Thus, in the diagrams, the electromagnetic current operator $j_\mu(0)$ is necessarily attached either to an internal line, representing an electrically charged particle, or to a vertex. We refer to these types of diagram as *type-1* and *type-2*, respectively. Schematic examples of both kinds of diagrams have been shown in Fig. 1.

Let us consider type-1 diagrams first, and denote their contribution to the vertex function as $\Gamma_\mu^{(1)}$. In each such diagram, we can always label the loop-integration momentum l in such a way that l is the momentum carried by the charged particle line outgoing from the electromagnetic vertex. A little thought reveals that, as a consequence, the line coming into the same vertex carries the momentum $l + P - P'$. The convention is represented in Fig. 1(a). Similarly, we consider a generic type-2 as shown in Fig. 1(b). Here, some of the external lines are attached to the photon vertex, and we denote by q the net momentum flowing into the diagram due to all these other external lines. In addition, we denote by $\tilde{P}$ and $\tilde{P}'$ the partial total momentum of the remaining incoming and outgoing lines,
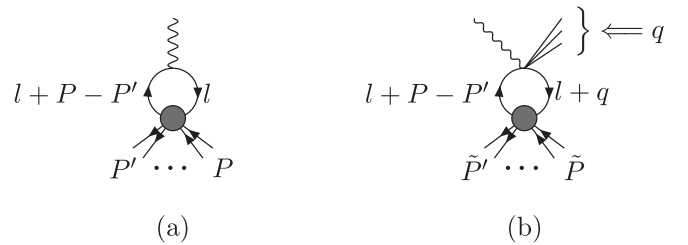

(a)   (b)

FIG. 1.   Schematic examples of (a) a type-1 diagram, and (b) a type-2 diagram, for the vertex function $\Gamma_\mu(p_i, p_f)$. The momentum variables are defined in the text.

so that $\tilde{P} - \tilde{P}' + q = P - P'$. Then, choosing the integration variable l such that the momentum carried by the internal line going into the vertex is again $l + P - P'$, it follows that the outgoing internal line has momentum $l + q$, as indicated in Fig. 1(b).

We now imagine constructing the amplitudes corresponding to each type of diagram. For each such amplitude, we define an auxiliary function by making the replacement

$$l + P - P' \rightarrow l - k, \qquad (3.11)$$

in the propagator (and the tree-level vertex function) of the internal charged line that goes into the electromagnetic vertex, where k is an arbitrary vector. We denote by $\bar{\Gamma}^{(1)}_\mu(p_i, p_f, k)$ the sum of the auxiliary functions corresponding to the type-1 diagrams, and similarly by $\bar{\Gamma}^{(2)}_\mu(p_i, p_f, k)$ the corresponding sum obtained in the same way for the type-2 diagrams. Furthermore, we define the total auxiliary vertex function as the sum

$$\bar{\Gamma}_\mu(p_i, p_f, k) = \bar{\Gamma}^{(1)}_\mu(p_i, p_f, k) + \bar{\Gamma}^{(2)}_\mu(p_i, p_f, k). \quad (3.12)$$

The function $\bar{\Gamma}_\mu(p_i, p_f, k)$ does not have a direct physical meaning, but by construction it is such that

$$\bar{\Gamma}_\mu(p_i, p_f, k)|_{k=P'-P} = \Gamma_\mu(p_i, p_f), \qquad (3.13)$$

which is the important relation for us in what follows.

We want to consider the process of Eq. (1.1). The off-shell amplitude in the presence of the external magnetic field, which is given by

$$\mathbb{M}^{(P)}_{i \rightarrow f}(p_i, p_f) = -i \int d^4x e^{i(P'-P)\cdot x} A^\mu(x) \Gamma_\mu(p_i, p_f), \tag{3.14}$$

can be expressed in terms of the auxiliary vertex function $\bar{\Gamma}_\mu(p_i, p_f, k)$ as

$$\mathbb{M}^{(P)}_{i \rightarrow f}(p_i, p_f) = -i \left[\int d^4x e^{ik\cdot x} A^\mu(x) \bar{\Gamma}_\mu(p_i, p_f, k) \right]_{k=P'-P}. \tag{3.15}$$

The same manipulations that we applied to Eq. (3.3) then leads us here to an equation that resembles Eq. (3.6),

$$\mathbb{M}^{(P)}_{i \rightarrow f}(p_i, p_f) = -\frac{1}{2}(2\pi)^4 \delta^4(P'-P) F^{\mu\nu}$$
$$\times \left\{ \frac{\partial}{\partial k^\nu} \bar{\Gamma}^{(1)}_\mu(p_i, p_f, k) \right.$$
$$\left. + \frac{\partial}{\partial k^\nu} \bar{\Gamma}^{(2)}_\mu(p_i, p_f, k) \right\}_{k=0}. \tag{3.16}$$

It should be remembered that we have been omitting all but the photon index in writing the $\bar{\Gamma}^{(1,2)}_\mu$, but in fact they are assumed to be present on both sides of this equation.

In spite of the similarity between the type-1 and type-2 contributions to this equation, there is an important differ-

ence between the two types which a closer look at Fig. 1 reveals clearly. If we denote generically by $\tilde{S}(p)$ the propagator of the internal line where the electromagnetic vertex is attached (whether it is a scalar, fermion of vector particle), then in type-1 diagrams that particular propagator appears in a combination that schematically looks like

$$\left[\frac{\partial}{\partial k} \tilde{S}(l) V \tilde{S}(l-k) \right]_{k=0}, \tag{3.17}$$

where V is a vertex factor. On the other hand, for type-2 diagrams the corresponding combination is

$$\left[\frac{\partial}{\partial k} \tilde{S}(l+q) V' \tilde{S}(l-k) \right]_{k=0}. \tag{3.18}$$

As we will show in the next section, in all cases, whether scalar, fermion, or vector particles, the combination given in Eq. (3.17) can be expressed in terms of the Schwinger propagator for a particle with momentum l, and that will allow us to prove the equivalence between the P-method calculation of the type-1 diagrams and the S-method. On the other hand, no such relation exists for the combination given in Eq. (3.18), which among other things depends not just on l but also on q. Therefore, in the process for which there are no type-2 diagrams, the P and the S methods are equivalent. But otherwise, the S-method does not yield the total amplitude. The type-2 diagrams of the P-method must be calculated separately to yield the total amplitude.

IV. EXAMPLE OF EQUIVALENCE OF THE TWO APPROACHES

We consider the P-method calculation of the neutrino self-energy in a background magnetic field. For the sake of simplicity, we will consider neutrino interactions with electrons only, which in the 4-Fermi approximation is given by

$$\mathcal{L} = \sqrt{2} G_F [\bar{e}\gamma_\mu (X + Y\gamma_5)e][\bar{\nu}\gamma^\mu L\nu]. \tag{4.1}$$

Here L is the projection operator for the left-chiral components of fermion fields, while X and Y stand for the weak coupling constants of the electron.

As explained in Sec. III A, in the P-method we start from the neutrino electromagnetic vertex function and then determine the B-dependent part of the self-energy by means of Eq. (3.8). In one-loop, the relevant diagram is depicted in Fig. 2, which in straightforward fashion yields

$$i\Gamma_\mu(p, p+k) = -\sqrt{2} G_F \gamma^\alpha L \int \frac{d^4l}{(2\pi)^4}$$
$$\times \text{Tr}[i\gamma_\alpha (X + Y\gamma_5)iS_0(l)ie\gamma_\mu iS_0(l-k)], \tag{4.2}$$

where, for the electron, we have used $Q = -1$. The k dependence of the vertex function comes only from the factor $S_0(l-k)$, and therefore using the relation
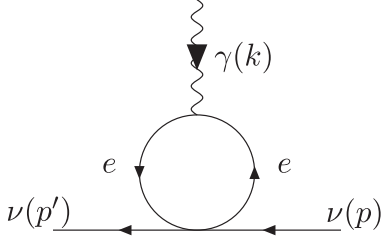
FIG. 2. Diagram for the off-shell vertex function of the neutrino. This is required for computing the background field-dependent contributions to neutrino self-energy in the perturbative approach.

$$\frac{\partial}{\partial k^\nu} S_0(l-k) = -\frac{\partial}{\partial l^\nu} S_0(l-k), \quad (4.3)$$

and taking the limit $k \to 0$, Eq. (3.8) yields

$$i\Sigma^{(P)} = \sqrt{2} G_F \gamma^\alpha L \frac{i}{2} F^{\mu\nu} \int \frac{d^4 l}{(2\pi)^4}$$

$$\times \text{Tr}\left[i\gamma_\alpha (X + Y\gamma_5) i S_0(l) i e \gamma_\mu \frac{\partial}{\partial l^\nu} i S_0(l) \right]. \quad (4.4)$$

In the S-method, the self-energy is determined to one-loop from the diagram shown in Fig. 3, using the Schwinger propagator for the internal electron line. In the linear approximation that we are considering, we use the linear formula for the propagator given in Eq. (2.13). Thus, denoting by $\Sigma^{(S)}$ the B-dependent part of the self-energy calculated in this way, we obtain

$$i\Sigma^{(S)} = -\sqrt{2} G_F \gamma^\alpha L \int \frac{d^4 l}{(2\pi)^4} \text{Tr}[i\gamma_\alpha (X + Y\gamma_5) i S_B(l)]. \quad (4.5)$$

Remembering Eq. (2.15), it follows that $\Sigma^{(S)}$ is identical to $\Sigma^{(P)}$ given in Eq. (4.4).

Looking closer at the two methods, we can see why they are equivalent in this case. In the P-method, the photon vertex appears between the two electron propagators in the combination

$$C_\mu(k, l) \equiv i S_0(l)(-ieQ\gamma_\mu) i S_0(l-k), \quad (4.6)$$

which, using Eq. (4.3), is seen to satisfy

$$-\frac{i}{2} F^{\mu\nu} \left[\frac{\partial}{\partial k^\nu} C_\mu(k, l) \right]_{k=0} = i S_B(l). \quad (4.7)$$
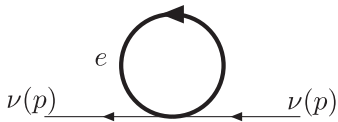

FIG. 3. Diagram for computing the neutrino self-energy in a magnetic field. The thick line indicates that the Schwinger propagator has to be used.

This Ward-like identity is the crucial relation that guarantees the equivalence of the two approaches. Diagrammatically, it can be represented in the form

$$(4.8)$$

where the lines at the bottom are external lines, the double line represents only the magnetic part of the propagator, and the blob denotes everything else in the diagram.

Let us now consider a more general amplitude that may involve diagrams in which the photon line, in the P-method, attaches to an internal scalar line. Denoting the charge of the scalar by eQ, the factor analogous to the one quoted in Eq. (4.6) would be in this case

$$C'_\mu(k, l) \equiv i\Delta_0(l)(-ieQ(2l_\mu - k_\mu)) i\Delta_0(l-k). \quad (4.9)$$

Although the electromagnetic coupling of the scalar is momentum dependent, it still follows that

$$-\frac{i}{2} F^{\mu\nu} \left[\frac{\partial}{\partial k^\nu} C_\mu^{(S)}(k, l) \right]_{k=0} = i\Delta_B(l), \quad (4.10)$$

as can be simply verified. Thus, the diagrammatic equation of Eq. (4.8) applies to this case as well. Furthermore, this conclusion is unchanged if the scalar mode is unphysical.

If the photon is attached to an internal W-boson line, the factor analogous to the one quoted in Eq. (4.6) is given by

$$C^{\lambda\rho}_{\ \mu}(k, l) \equiv i D_0^{\alpha\lambda}(l)(ie O_{\mu\alpha\beta}(k, l-k)) i D_0^{\beta\rho}(l-k), \quad (4.11)$$

where the $O_{\mu\alpha\beta}$ is defined in Eq. (2.28). Using the analog of Eq. (4.3) for the W propagator, we can write

$$\lim_{k\to 0} \frac{\partial}{\partial k^\nu} C^{\lambda\rho}_{\ \mu} = -ie D_0^{\alpha\lambda}(l) \lim_{k\to 0} \frac{\partial}{\partial k^\nu}$$

$$\times [O_{\mu\alpha\beta}(k, l-k) D_0^{\beta\rho}(l-k)]$$

$$= -ie D_0^{\alpha\lambda}(l) \left[-O_{\mu\alpha\beta}(0, l) \frac{\partial}{\partial l^\nu} \right.$$

$$\left. + \left(\frac{\partial}{\partial k^\nu} O_{\mu\alpha\beta}(k, l-k) \right)_{k=0} \right] D_0^{\beta\rho}(l), \quad (4.12)$$

and by direct computation using Eq. (2.28) it follows that

$$\frac{\partial}{\partial k^\nu} O_{\mu\alpha\beta}(k, l-k) = -\eta_{\mu\nu}\eta_{\alpha\beta} - (2-\zeta)\eta_{\nu\alpha}\eta_{\mu\beta}$$

$$+ 2\eta_{\alpha\mu}\eta_{\nu\beta}. \quad (4.13)$$

Therefore, contracting with the antisymmetric tensor $F^{\mu\nu}$,

we obtain

$$-\frac{i}{2}F^{\mu\nu}\left[\frac{\partial}{\partial k^{\nu}}C^{\lambda\rho}{}_{\mu}\right]_{k=0}=iD_B^{\lambda\rho}, \qquad (4.14)$$

which proves the equivalence also when the photon is attached to a W-boson line. Notice that we have exhausted all the possible ways in which the photon, in the P-method, can be attached to an internal line in a diagram since, as emphasized earlier, there is no $W\phi$-photon trilinear coupling in the gauge chosen for the W's.

This completes the proof that there is a one-to-one correspondence between the diagrams in the S-method, and the type-1 diagrams in the P-method, in which the photon appears attached to the internal lines of the diagram. Therefore, for transition amplitudes for which there are no contributions from type-2 diagrams, both methods give equivalent results. However, as we will see next, there are amplitudes for which the P-method involve the type-2, diagrams which have no counterpart in the S-method.

V. EXAMPLES OF NONEQUIVALENCE OF THE TWO APPROACHES

A. Processes involving charged gauge bosons

Let us consider the amplitude for the process

$$Z(p)\overset{B}{\longrightarrow}\nu(p_1)\bar{\nu}(p_2), \qquad (5.1)$$

and focus the attention on the modification to the tree-level, B-independent, term due to the background magnetic field. Without any of the essential features that are important for us, we can simplify the discussion by assuming that the neutrinos are massless, so that there is no neutrino mixing, and the final state contains the electron neutrino and its antiparticle. The one-loop diagrams which contribute to the amplitude are shown in Fig. 4, where the internal fermion lines represent the electron.

In the S-method, the Schwinger propagators must be used for the internal lines in these diagrams. In the linear approximation that we are using, we need to consider the B-dependent part of the propagator of each line at a time.

On the other hand, in the P-method, the diagrams are all those that can be obtained by attaching a photon to each diagram of Fig. 4, in all possible ways. For example, Fig. 5 shows all the possible ways in which a photon line can be attached to the diagram of Fig. 4(a). From the discussion of Sec. IV, and, in particular, by means of the identity in Eq. (4.14), it follows that the P-method evaluation of diagram (a3) of Fig. 5 yields a result that is identical to the contribution that comes from the B-dependent part of the W-boson propagator in the S-method evaluation of Fig. 4(a). Similarly, Eq. (4.7) implies that the P-method calculation of the diagrams (a1) and (a2) of Fig. 5 is identical to the contribution from the B-dependent part of the electron propagator in the S-method evaluation of Fig. 4(a). In summary, the S-method evaluation of
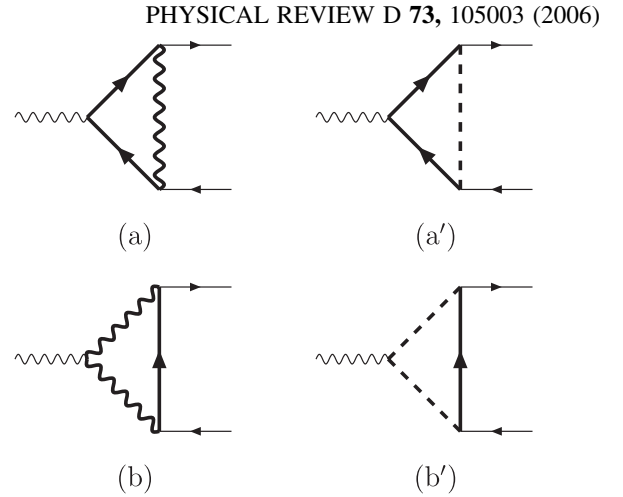

FIG. 4. One-loop diagrams for the process $Z \to \nu\bar{\nu}$. The internal solid, wavy, and dashed lines represent the electron, the W-boson, and the unphysical charged Higgs, respectively. In the S-method, we should take Schwinger propagators for the thick lines.

Fig. 4(a), and the P-method evaluation of the diagrams (a1), (a2), and (a3) of Fig. 5, yield the same result. The same conclusion holds for Fig. 4(a′) and the corresponding diagrams of the P-method, since in the latter set of diagrams the photon is attached to an internal line, and the identities in Eqs. (4.7), (4.10), and (4.14) can be invoked once again.

In the terminology that we have used, the P-method diagrams that we had to consider so far are type-1 diagrams. The situation with diagrams Fig. 4(b) and 4(b′) is different because, in addition to the possibility of attaching the photon line to each of the internal lines, that does not exhaust all possibilities. For example, in Fig. 4(b), an extra photon line can be added to the WWZ vertex, turning it into a $WWZ\gamma$ vertex. The same can be done to the diagram in Fig. 4(b′) as well. The resulting diagrams, shown in Fig. 6, have no counterpart in the Schwinger method. In our terminology, they are type-2 diagrams.

We are not showing the type-1 diagrams that correspond to the S-method evaluation of Figs. 4(b) and 4(b′), since they are similar to those shown in Fig. 5 and, from the arguments of Sec. IV, it follows that the evaluation of the corresponding diagrams in the two methods gives the same result once again.
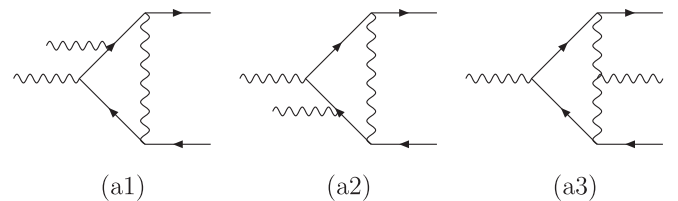

FIG. 5. 1-loop diagrams for the process $Z + \gamma \to \nu\bar{\nu}$ obtained by attaching a photon line to the diagram of Fig. 4(a).

To complete the demonstration of nonequivalence of the two methods, we now need to show that the contribution of the type-2 diagrams shown in Fig. 6 is nonvanishing. Following the prescription for constructing the auxiliary amplitudes that correspond to the diagrams, we can write them in the form

$$-i\bar{\Gamma}_{\mu\nu}^{(bx)} = \left(\frac{ig}{\sqrt{2}}\right)^2 \int \frac{d^4l}{(2\pi)^4} [\gamma_\alpha L i S_0(p - p_2 - l)\gamma_\beta L]$$
$$\times iD_0^{\alpha\sigma}(l + k)iD_0^{\beta\tau}(l - p)iQ_{\sigma\tau\mu\nu}, \quad (5.2)$$

$$-i\bar{\Gamma}_{\mu\nu}^{(b'x)} = \left(\frac{igm_e}{\sqrt{2}M_W}\right)^2 \int \frac{d^4l}{(2\pi)^4} [LiS_0(p - p_2 - l)R]$$
$$\times i\Delta_0^{(W)}(l + k)i\Delta_0^{(W)}(l - p)iQ_{\mu\nu}, \quad (5.3)$$

where the propagators of the W-boson and the unphysical charge Higgs boson are given in Eqs. (2.39) and (2.42). In addition, we have denoted by $Q_{\sigma\tau\mu\nu}$ and $Q_{\mu\nu}$ the quartic couplings of the $Z\gamma$ with WW and the unphysical Higgs which, in the gauge introduced in Eq. (2.26), are given by

$$Q_{\sigma\tau\mu\nu} = -eg\cos\theta_W(2\eta_{\sigma\tau}\eta_{\mu\nu} - \eta_{\sigma\mu}\eta_{\tau\nu} - \eta_{\sigma\nu}\eta_{\tau\mu}),$$
$$Q_{\mu\nu} = \frac{eg\cos2\theta_W}{\cos\theta_W}\eta_{\mu\nu}, \quad (5.4)$$

respectively. From Eq. (3.16), it then follows that these diagrams give the following contribution to the amplitude $Z \to \nu\bar{\nu}$ amplitude given by

$$\Gamma_\mu^{(x)} = -\frac{i}{2}F^{\nu\lambda}\left[\frac{\partial}{\partial k^\lambda}\Gamma_{\mu\nu}^{(bx+b'x)}\right]_{k=0}$$
$$= -\frac{g^2}{4}F^{\nu\lambda}\int\frac{d^4l}{(2\pi)^4}\left[[\gamma_\alpha LS_0(p_1 - l)\gamma_\beta L]\right.$$
$$\times \frac{\partial D_0^{\alpha\sigma}(l)}{\partial l^\lambda}D_0^{\beta\tau}(l - p)Q_{\sigma\tau\mu\nu} + \left(\frac{m_e}{M_W}\right)^2$$
$$\times [LS_0(p_1 - l)R]\frac{\partial\Delta_0^{(W)}(l)}{\partial l^\lambda}\Delta_0^{(W)}(l - p)Q_{\mu\nu}\bigg],$$
$$(5.5)$$

where we have made use of relations analogous to Eq. (4.3). Certainly, this contribution is nonvanishing. It also shows the general structure displayed in Eq. (3.18),
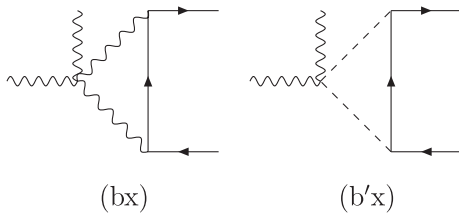

(bx)   (b'x)

FIG. 6.   1-loop diagrams for the process $Z + \gamma \to \nu\bar{\nu}$, obtained by attaching a photon line to the Z vertices of the diagrams of Fig. 4(b) and 4(b?).

where the two propagators appear with different momenta despite the fact that the external photon momentum has been set to zero.

B. Theory with linearized gravity

In the linear theory of gravity, the couplings of the graviton with the matter and gauge fields can be determined by writing the space-time metric in the form

$$g_{\lambda\rho} = \eta_{\lambda\rho} + 2\kappa h_{\lambda\rho}, \quad (5.6)$$

where $h_{\lambda\rho}$ is identified with the graviton field, and then expanding the couplings in the Lagrangian up to the linear order in κ. The constant κ is defined in terms of Newton's gravitational constant by

$$\kappa = \sqrt{8\pi G}, \quad (5.7)$$

which is such that the field $h_{\lambda\rho}$ has the properly normalized kinetic energy term in the Lagrangian. This point of view for treating processes involving the gravitational and standard model interactions is the same as that employed in some recent works for the calculation of quantum gravity amplitudes [18–20], in which general relativity is treated as an effective field theory for energies below the Planck scale [21,22].

The interaction Lagrangian so obtained contains vertices involving both the photon and graviton that give rise to type-2 diagrams when we consider processes involving gravitons in the presence of a B field. In order to make the discussion concrete, we consider the process

$$\nu_1 \xrightarrow{B} \nu_2 + \mathcal{G}, \quad (5.8)$$

where $\mathcal{G}$ is the graviton, and ν_1, ν_2 are two different neutrino eigenstates. The couplings involving gravitons that are relevant to this process have been deduced in the literature [23–27]. We do not reproduce them here since we will not carry out the calculation of the amplitude for this process. We will limit ourselves to indicate the diagrams that are relevant for such a calculation using the two methods that we have considered.

In the absence of the B field, the amplitude is determined from the diagrams shown in Fig. 7, the tree-level contribution being zero due to the fact that the gravitational couplings are flavor diagonal and universal. The process cannot occur in the vacuum because of angular momentum conservation. But in the background B field, this obstruction is lifted. We can then try to calculate the amplitude of the process by interpreting the charged fermion propagators of Fig. 7 as Schwinger propagators. Further, although the internal loop can contain all charged leptons, we can imagine considering only the contributions for the electron in the loop, with the understanding that restoring the contributions of the muon and the tau can be made in analogous fashion. Carrying out the calculation in this way is the prescription of the S-method.
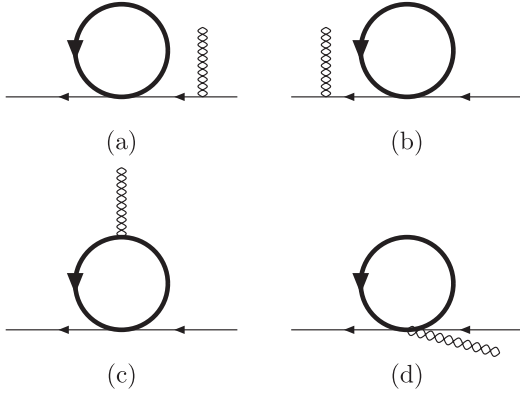
FIG. 7.   One-loop diagrams for the process $\nu_1 \rightarrow \nu_2 + G$ in the four-Fermi interaction approximation.

Let us now shift our attention to the P-method and look at the process

$$\nu_1 + \gamma \rightarrow \nu_2 + G, \qquad (5.9)$$

for which the relevant diagrams are shown in Fig. 8. Clearly, diagrams (a)–(d) contain the usual QED vertex for the electron and therefore the factor C_μ given in Eq. (4.6). The calculation of the amplitudes of these diagrams yields the same result as that obtained from the S-method calculation of the diagrams of Fig. 7.

However, the contribution of the type-2 diagrams (e) and (f) of Fig. 8 have no counterpart in the S-method. If we do not consider their contribution to the total amplitude, then if we consider the process of Eq. (5.9) as a physical process involving a real photon, the amplitude does not satisfy the
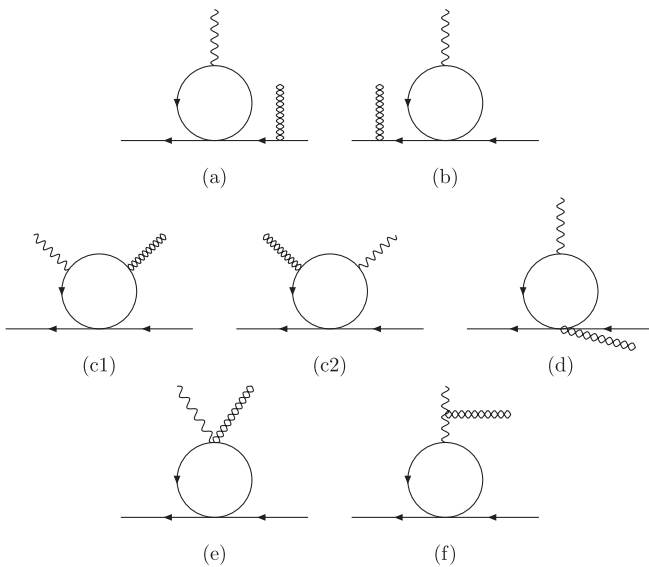

FIG. 8.   One-loop diagrams for the $\nu_1 + \gamma \rightarrow \nu_2 + G$ process in the 4-Fermi approximation. In our terminology, the diagrams (a)–(d) are type-1 diagrams while (e) and (f) are type-2.

transversality requirements due to the gravitational and electromagnetic gauge invariance. Moreover, the total amplitude, taking those two diagrams into account does satisfy the aforementioned conditions. We have verified this explicitly. This reinforces our conclusion that the S-method does not yield the total amplitude in those cases in which the P-method involves type-2 diagrams.

VI. CONCLUSIONS

In this work we have considered the calculation of amplitudes for processes that take place in a constant background magnetic field B with the purpose of comparing two methods. One, to which we refer as the P-method, uses the standard method for the calculation of an amplitude in an external field. The other, the S-method, utilizes the Schwinger propagator for charged particles in a magnetic field.

We showed that there are processes for which the two methods of calculating the amplitude yield equivalent results. We illustrated this with the specific example of the neutrino forward scattering amplitude in a magnetic field, and we indicated specifically the propagator identities that operate to guarantee the equivalence in that case.

However, we pointed out that there are processes for which the Schwinger-propagator method does not yield the total amplitude. For illustrative purposes, we considered the amplitude for Z decay into a neutrino-antineutrino pair in a B field, in the context of the standard model. In that case, the diagrams that must be included in the P-method of calculation can be divided in two groups, that we called type-1 and type-2 diagrams. In the type-1 diagrams the electromagnetic vertex is attached to an internal propagator line, while in type-2 diagrams there are some external lines as well attached to that vertex. We showed that there is a one-to-one correspondence between the diagrams of the S-method and the type-1 diagrams of the P-method and that their calculations yield the same result. Therefore, for processes for which the type-2 diagrams do not exist, both the P and S methods yield the same result, which is the case of the neutrino processes that we have mentioned. However, the type-2 diagrams have no counterpart in the S-method and therefore this method does not yield the complete amplitude. The total amplitude is obtained by taking the result of the type-1 diagrams, which can be calculated by either method, and then adding the result of the type-2 diagrams using the P-method.

Moreover, we indicated that leaving out the type-2 diagrams in the calculation of the amplitude does not yield a gauge-invariant result. We have verified this explicitly by considering the neutrino decay into another neutrino and a graviton in a B field, which is another process for there are type-2 diagrams. In that particular case, we also verified that by including the type-2 diagrams the gauge invariance of the amplitude is restored, which reinforces our conclusion that the S-method does not yield the total amplitude in

the general case in which the P-method contains type-2 diagrams.

Needless to say, in the original context of the Schwinger propagator, namely, QED, there are no type-2 diagrams, so that both methods are equivalent. However, the situation is different when the other particles and interactions of the standard model are taken into account, and/or possibly the gravitational interactions as well. Our remarks should be taken within these broader contexts.

As already mentioned, when these types of processes occur in the environments of realistic astrophysical systems, the effects of the background must be included. The method that we have presented here for the calculation of such amplitudes can be extended to the framework of finite temperature field theory to include the effects of the background medium. The application of these methods in such contexts will be presented separately.

[1] S. Esposito and G. Capone, Z. Phys. C **70**, 55 (1996).
[2] P. Elmfors, D. Grasso, and G. Raffelt, Nucl. Phys. **B479**, 3 (1996).
[3] A. N. Ioannisian and G. G. Raffelt, Phys. Rev. D **55**, 7038 (1997).
[4] A. Erdas, C. W. Kim, and T. H. Lee, Phys. Rev. D **58**, 085016 (1998).
[5] A. K. Ganguly, S. Konar, and P. B. Pal, Phys. Rev. D **60**, 105014 (1999).
[6] K. Bhattacharya, A. K. Ganguly, and S. Konar, Phys. Rev. D **65**, 013007 (2002).
[7] For a review and extensive references, see, e.g., K. Bhattacharya and P. B. Pal, Proc. Indian Natl. Sci. Acad., Part A **70**, 145 (2004).
[8] T. M. Tinsley, Phys. Rev. D **65**, 013008 (2002).
[9] J. F. Nieves, Phys. Rev. D **68**, 113003 (2003).
[10] K. Bhattacharya and A. K. Ganguly, Phys. Rev. D **68**, 053011 (2003).
[11] J. F. Nieves, Phys. Rev. D **70**, 073001 (2004).
[12] J. C. D'Olivo, J. F. Nieves, and P. B. Pal, Phys. Rev. D **40**, 3679 (1989).
[13] J. S. Schwinger, Phys. Rev. **82**, 664 (1951).
[14] A. Erdas and G. Feldman, Nucl. Phys. **B343**, 597 (1990).
[15] K. Bhattacharya, Ph.D. thesis, Jadavpur University [hep-ph/0407099]. See, in particular, Appendix B.
[16] K. Bhattacharya, hep-ph/0510280.
[17] K. Fujikawa, Phys. Rev. D **7**, 393 (1973).
[18] N. E. J. Bjerrum-Bohr, J. F. Donoghue, and B. R. Holstein, Phys. Rev. D **67**, 084033 (2003); **71**, 069903(E) (2005).
[19] N. E. J. Bjerrum-Bohr, J. F. Donoghue, and B. R. Holstein, Phys. Rev. D **68**, 084005 (2003); **71**, 069904(E) (2005).
[20] J. F. Nieves and P. B. Pal, Phys. Rev. D **72**, 093006 (2005).
[21] J. F. Donoghue, Phys. Rev. D **50**, 3874 (1994).
[22] C. P. Burgess, Living Rev. Relativity **7**, 5 (2004).
[23] S. Y. Choi, J. S. Shim, and H. S. Song, Phys. Rev. D **51**, 2751 (1995).
[24] J. S. Shim and H. S. Song, Phys. Rev. D **53**, 1005 (1996).
[25] J. F. Nieves and P. B. Pal, Phys. Rev. D **58**, 096005 (1998).
[26] J. F. Nieves and P. B. Pal, Mod. Phys. Lett. A **14**, 1199 (1999).
[27] J. F. Nieves and P. B. Pal, Phys. Rev. D **63**, 076003 (2001).